Planta (2025) 262:123
https://doi.org/10.1007/s00425-025-04840-9

ORIGINAL ARTICLE

Insight into the genetic network governing long-stalked glandular trichome development in *Nicotiana tabacum*

Alice Berhin[1] · Aldana Ramirez[1] · Manon Peeters[1] · Gabriel Walckiers[1] · Maxime Vannieuwenhuyze[1] · Sylvain Legay[2] · Belkacem El Amraoui[1] · Charles Hachez[1]

Received: 10 March 2025 / Accepted: 28 September 2025

Abstract

Main conclusion **Using a transcriptional switch-based approach in *Nicotiana tabacum*, we identified key regulatory factors that control long-stalked trichome development. Our results highlight candidate genes implicated in glandular trichome formation and establish a foundation for future research on trichome development.**

Abstract Glandular trichomes play a pivotal role in plant defense against various biotic and abiotic stresses. To unravel the genetic network driving glandular trichome development in *Nicotiana tabacum*, we employed a transcriptional switch-based approach using heterologous expression of AmMIXTA, a MYB transcription factor from *Antirrhinum majus*. Through comprehensive RNA-seq analysis of transgenic tobacco seedlings where long-stalked glandular trichome development was induced in aerial parts, we identified a suite of differentially expressed genes, including several transcription factors, shedding light on the early transcriptional cascade governing this developmental process. Moreover, through confocal live cell imaging of transcriptional reporter lines, interaction studies and DAP-seq assays, we confirmed the involvement of *NtZFP8*, a gene identified in our study, in long-stalked glandular trichome development. Our findings support a model in which *NtZFP8* regulates a gene network essential for this developmental process. This study underscores the effectiveness of our approach in decoding the regulatory landscape of glandular trichome development in *N. tabacum* and provides a valuable framework for future functional investigations.

Keywords C2H2 zinc finger protein · Developmental biology · MYB transcription factor · Solanaceae · Trichome · ZFP8

Abbreviations

DEGs Differentially expressed genes
ZFP Zink finger protein

Introduction

Trichomes, which are epidermal outgrowths found on the aerial parts of many plant species, display an incredible variety of structures, from simple single cells to complex, multicellular forms that are frequently topped with a glandular head (Hauser 2014). Trichomes play an essential role in plant environmental adaptation by acting as physical barriers against a variety of biotic and abiotic stresses such as excessive sunlight (UV radiation), drought or attacks by pathogens or insects. Furthermore, glandular trichomes produce and store or secrete a diverse array of secondary metabolites—such as acyl sugars, terpenoids, phenylpropanoids, flavonoids, and alkaloids—serving as a chemical line of defense against herbivores and pathogens, and/or to attract pollinators (Gershenzon and Dudareva 2007; Huchelmann et al. 2017). By enhancing plants resistance to stresses, glandular trichomes contribute to plant survival and reproductive fitness (Hauser 2014).

Communicated by Dorothea Bartels.

✉ Charles Hachez
charles.hachez@uclouvain.be

[1] Louvain Institute of Biomolecular Science and Technology, UCLouvain, Louvain-La-Neuve, Belgium

[2] Environmental Research and Innovation, Luxembourg Institute of Science and Technology, Esch-Sur-Alzette, Luxembourg

Published online: 15 October 2025

In the model plant *Arabidopsis thaliana*, significant progress has been made in understanding the genetic framework governing the development of non-glandular, unicellular branched trichomes, unveiling an extensive network of key regulatory genes. Its genetic basis is managed by a complex of R2R3 MYB/bHLH/WD-repeat transcription factors regulating trichome initiation and morphogenesis: GLABRA1 (AtGL1), GLABRA3 (AtGL3)/ENHANCER OF GLABRA3 (AtEGL3), and TRANSPARENT TESTA GLABRA1 (AtTTG1). For a comprehensive review, refer to Han et al. (2022).

Compared to unicellular trichomes, the genetic basis of multicellular trichome development is less understood but shows ongoing progress (Hauser 2014; Chalvin et al. 2020). Developmental regulation involves multiple genes and regulatory pathways, varying widely among plant species and trichome types (non-glandular vs glandular, multicellular vs unicellular) and highlights their diversity of evolutionary origin (Hauser 2014; Chalvin et al. 2020). This complexity hinders the creation of a universal model for understanding the genetic factors in glandular trichome development. Unlike *Arabidopsis thaliana*, which provides a unified model for single-cell trichome study, different species or groups serve as models to understand the genetic control behind specific glandular trichome types, such as Lamiaceae for peltate trichomes or Solanaceae for capitate trichomes (Tissier 2012).

Our research aims to unravel the transcriptional networks governing the development of these epidermal structures, particularly in *Nicotiana tabacum*, belonging to the agronomically important Solanaceae family in the Asterid clade. This plant possesses three multicellular trichome types: short-stalked glandular trichomes, non-glandular trichomes and long-stalked glandular trichomes (Meyberg et al. 1991; Uzelac et al. 2021).

Numerous transcription factors are implicated as regulators of multicellular trichome development across Asterid species, indicating the genetic intricacy controlling the development of these structures (Han et al. 2022): (1) MYB transcription factors such as AaMIXTA and AaMYB1 in *Artemisia annua* (Matias-Hernandez et al. 2017; Shi et al. 2017), AmMIXTA, AmMYBML1, and homologs of AaMIXTA, in *Antirrhinum majus*, SlMX1 in *Solanum lycopersicum* (Ewas et al. 2016; Wu et al. 2023), NbMYB123 in *Nicotiana benthamiana* (Liu et al. 2018), McMIXTA in *Mentha canadensis* (Qi et al. 2022) and GLAND CELL REPRESSOR (SlGCR1 and SlGCR2) (Chang et al. 2024); (2) C2H2 zinc-finger (ZFP) transcription factors such as SlHAIR, SlZFP6, SlZFP8/SlHAIR2 (Chang et al. 2018; Zheng et al. 2021) and GLABROUS INFLORESCENCE STEM (NbGIS) (Liu et al. 2018); (3) bHLH transcription factors such as SlMYC1 (Xu et al. 2018); (4) homeodomain-leucine zipper (HD–ZIP) IV transcription factors like AaHD1, AaHD8 (Yan et al. 2017, 2018), SlCD2, homolog of AaHD8 (Nadakuduti et al. 2012), SlWOOLLY and NbWOOLLY (Yang et al. 2011, 2015); (5) WRKY transcription factors such as AaGSW2 (Xie et al. 2021); (6) AP2/ERF transcription factors such as LEAFLESS (SlLFS) and SlTOE1B (Wu et al. 2023; Chang et al. 2024); (7) WUSCHEL-related homeobox such as SlWOX3 (Wu et al. 2023); (8) TOESINTE BRANCHED, CYCLOIDEA, and PROLIFERATING CELL NUCLEAR ANTIGEN BINDING FACTOR transcription factor (TCP) like BRANCHED2a (SlBRC2a) (Wu et al. 2024a). Additionally, cell cycle regulators, like E3 ubiquitin ligase (SlMTR1/SlCYCB2 and SlMTR2, NbCYCB2 and NtCYCB2) impact trichome development, emphasizing the sophisticated control of cell division and differentiation needed for multicellular trichome architecture in Solanaceae (Gao et al. 2017; Wu et al. 2020, 2023; Wang et al. 2021).

Recent studies in tomato underscore the pivotal role of HD–ZIP transcription factors in determining trichome cell fate, revealing a regulatory landscape distinct from that of unicellular trichome development (Wu et al. 2023, 2024a, b). Indeed, SlWOOLLY controls trichome development in a dosage-dependent mechanism controlled by self-activating and SlMTR1-mediated feedback. Trichome type fate is then controlled by SlWOX3 and SlMX1 for digitate trichomes and SlLFS for peltate trichomes; high levels of SlWOOLLY preferentially activate the SlWOX3/SlMX1 complex, which inhibits *SlLFS* expression (Wu et al. 2023). When *SlWOOLLY* expression level is low, SlBRC2a mediates a negative feedback loop, transitioning cells from division to expansion (Wu et al. 2024a). In addition, SlGCR1/SlGCR2 operate dose-dependently in the apical cell to regulate glandular head formation (Chang et al. 2024); SlTOE1B inhibits *SlGCRs* expression whose low expression level activates *SlLFS* leading to gland formation (Chang et al. 2024).

In *N. tabacum*, glandular trichome development is regulated through a transcriptional pathway differing from the regulatory mechanisms controlling the formation of unicellular non-glandular trichomes (Glover et al. 1998; Payne et al. 1999; Perez-Rodriguez et al. 2005). In *A. majus*, AmMIXTA regulates cell wall deposition in floral papillae (Noda et al. 1994). Ectopic expression of *AmMIXTA* induces the formation of multicellular trichomes in *N. tabacum*, demonstrating the involvement of R2R3 MYB transcription factors in the development of glandular trichomes (Glover et al. 1998; Payne et al. 1999; Perez-Rodriguez et al. 2005).

By using inducible *AmMIXTA* expression as a switch to trigger long-stalked glandular trichome formation in a normally trichome-free organ such as the cotyledon, this exploratory study opens new avenues for investigating the molecular mechanisms that initiate and shape early genetic events in glandular trichome development in tobacco. Our work provides a broader framework for understanding the

initiation of glandular trichome development in *N. tabacum* and identifies potential candidate genes for future research in this field.

Material and methods

Genetic constructs

The *AmMIXTA* coding sequence was provided by Prof. Beverley Glover (University of Cambridge, UK). This sequence was amplified (Table S1), cloned into a *pENTR/D-TOPO* entry vector (Invitrogen, 45-0218) and transferred to a *pMDC7* destination vector containing a β-estradiol promoter (Curtis and Grossniklaus 2003) using Gateway Technology (Life Sciences). The *NtZFP8* (LOC107828820) coding sequence was amplified by PCR from cDNA generated based on leaf primordia mRNA (Table S1), and recombined into a *pDONR221* vector to create the *pENTRY L1-NtZFP8-L2*. *p35S::NtZFP8* was produced by LR Gateway reaction recombining the corresponding entry clone into the *pH7WG2D* (Karimi et al. 2002). A 1982 bp fragment upstream of the *NtZFP8* coding sequence was cloned into *pDONR L4-L1r* to produce *pENTRY L4-pNtZFP8-R1*, a fragment of 1927 bp for *NtGL2* to *pENTRY L4-pNtGL2-R1* and a fragment of 3191 bp for *NtJACKDAW* to *pENTRY L4-pNtJACKDAW-R1*. *pZFP8::nlsGFP-GUS, pGL2::nlsGFP-GUS* and *pJACKDAW::nlsGFP-GUS* were generated by recombining *pENTRY L4-pNtZFP8-R1* with *pENTRY L1-nlsGFPGUS-L2* into *pH7m34GW* (Karimi et al. 2002; Berhin et al. 2019). For yeast two-hybrid assays, coding sequences of *NtZFP8, AmMIXTA,* and *nls-GFP* were PCR-amplified using primers with BsaI site overhangs (Table S1) and cloned into CK011 and CK012, containing respectively the GAL4 activation and binding domain, under the *ADH1* promoter (Gantner et al. 2018), using Golden Gate cloning technology (Kirchmaier et al. 2013). For protein expression in DAP-seq, *pENTRY L1-NtZFP8-L2, pENTRY L1-AmMIXTA-L2*, and *pENTRY L1-nlsGFP-L2* were transferred to the *pIX-HALO* plasmid via an LR Gateway reaction, resulting in *pIX::HALO-NtZFP8, pIX::HALO-AmMIXTA,* and *pIX::HALO-nlsGFP* constructs (Bartlett et al. 2017). For recombinant protein expression, the coding sequence of both genes were amplified (Table S1) and cloned into pQE60 (Qiagen) using Mlu1 and BamHI restriction sites. For the dual luciferase reporter assay system, the coding sequences of the luciferase (LUC) and renilla luciferase (REN) reporter genes were PCR amplified from the *pGWL7* and *pGB109* plasmids (respectively) and recombined by BP reaction into a *pDONR221* donor-vector to create the *pENTRY L1-LUC-L2* and *pENTRY -L1-REN-L2* plasmids. The reporter control plasmid *p35S::REN*, the promoter reporter plasmids *pNtJACKDAW::LUC* and *pNtGL2::LUC*, and the protein expression plasmids *pUBQ::nlsGFP, pUBQ::AmMIXTA* were all generated by LR reaction by recombination of their promoter elements *(pENTRY L4-p35S-R1; pENTRY L4-pNtJACKDAW-R1; pENTRY L4-pNtGL2-R1; pENTRY L4-pAtUBQ10-R1)* with their corresponding coding sequence element *(pENTRY L1-REN-L2; pENTRY L1-LUC-L2; pENTRY L1-nlsGFP-L2; pENTRY L1-AmMIXTA-L2)* into the *pH7m24GW* destination plasmid.

For the BIFC, coding sequences of *AmMIXTA* and *NtZFP8* were amplified (Table S1) and cloned via BP Gateway reaction into a *pDONR-R1R4* and *pDONR-R3R2,* respectively. Then they were transferred together via LR reaction into the *pBiFCt-2in1-NN* expression vector (Grefen and Blatt 2012).

Plant material and growth conditions

Nicotiana tabacum L. cv Petit Havana SR1 was used for stable plant transformation. Seeds were surface-sterilized with chlorine gas, sown on half-strength Murashige and Skoog agar plates (MP Biochemicals, 92,610,024), stratified at 4 °C for 3 days, and subsequently transferred to a growth chamber (16 h light/8 h dark, 50 µmol photon m^{-2} s^{-1}, 25 ± 2 °C). Seedlings from in vitro cultures were then transferred to Jiffy pots for a week or germinated in Jiffy pots for 2 weeks before moving to pots with soil in a phytotron (25 °C, 16 h photoperiod, 200 µmol photon m^{-2} s^{-1}) for propagation and phenotyping. All constructs for plant transformation were introduced into *Agrobacterium tumefaciens* strain GV3101pmp90 and transformed into tobacco using a leaf disk method modified from Horsh et al. (1985). Transgenic lines carrying *pEST::AmMIXTA*, *p35S::NtZFP8*, *pNtZFP8::nlsGFP-GUS*, *pNtGL2::nlsGFP-GUS* and *pNtJACKDAW::nlsGFP-GUS* were generated. Experiments with AmMIXTA were performed on T2 generation while the ones with ZFP8 were conducted on T1.

mRNA extraction

For the RNA-seq, aerial parts of 15 seedlings were harvested per sample per condition. To study *NtZFP8* expression, various tissues from 6-week-old plants were used, including leaf primordia (< 1.5 cm), young leaves (± 10 cm), mature leaves (± 20 cm), and mature trichomes. For each of the harvested tissues, tissues from three plants were mixed to form a sample and four samples were harvested to have four biological replicates. For the overexpressing lines of *NtZFP8*, three disks from the same leaf used for trichome density were harvested from three independent plants. RNA was extracted using the Spectrum Plant Total RNA Kit with on-column DNase I digestion. One µg RNA was reverse transcribed and analyzed by RT-qPCR with specific primers (Table S1). Normalization was done by geometric averaging of *NtEF2α*,

NtACTIN and *NtUBC2* (Vandesompele et al. 2002). Relative expression levels were calculated using the $2^{-\Delta\Delta CT}$ method (Schmittgen and Livak 2008).

RNA-sequencing

Seedlings from independent T1 lines expressing *AmMIXTA* were screened for trichome proliferation by germinating them on 1/2 MS medium, with 10 µM β-estradiol and checking *AmMIXTA* expression level via RT-qPCR. Selected T2 seeds were grown under control and β-estradiol conditions for 7 days. Aerial parts from 15 seedlings were collected at 4 and 48 h post-induction for mRNA extraction (see above).

RNA-seq libraries were generated and sequenced by Genewiz (Azenta Life Science) using Illumina NovaSeq sequencing platform, yielding at least 38 million 150 bp paired-end reads per sample (Table S2). Reads were cleaned, trimmed, and mapped to the *N. tabacum* TN90 reference genome (Sierro et al. 2014) using CLC Genomic Workbench. Differentially expressed genes (DEGs) were identified based on normalized counts per million (CPM), with a fold change > 1.5 (upregulated genes) or < 0.67 (downregulated genes) and a $P < 0.05$, using EdgeR in RStudio (Law et al. 2016).

DEGs were analyzed for enriched Gene Ontology (GO) terms using PANTHER classification system (Mi et al. 2019; Thomas et al. 2022) and visualized with rrvgo (Sayols 2023).

DNA Affinity purification sequencing (DAP-seq)

DNA from three 6-week-old plant leaf primordia was extracted using the Wizard Genomic DNA Purification Kit (Promega). The DAPseq experiment followed Bartlett et al. (2017)'s protocol. HALO-AmMIXTA, HALO-NtZFP8 and HALO-nlsGFP (negative control) were each expressed three times using the TnT® Coupled Wheat Germ Extract System (Promega, L41030). Index and adaptor were added to the DNA fragments using NEBNext® Multiplex Oligos for Illumina® primers (NEB, E6440S). DNA-seq libraries were sequenced by Macrogen using Illumina NovaSeq 6000 platform yielding at least 50 million 150 bp paired-end reads (Table S3). Reads were cleaned and mapped (see RNA-seq). Peak scores (> 2) and P (< 0.05) were calculated using the Transcription Factor CHIP-seq tool from CLC Genomic Workbench comparing our samples to the negative control (DNA bound to nlsGFP). Peaks of interest were selected based on their proximity to a gene: 3 kb upstream of a START codon and 1 kb downstream of a STOP codon.

Microscopy and phenotyping

Trichomes were observed using an Observer Z1 microscope. GFP signals in reporter lines were imaged with a Stellaris 8 Falcon confocal microscope (excitation: 488 nm for GFP, 453 nm for chlorophyll; detection: 500–550 nm for GFP, 620–750 nm for chlorophyll b). For BiFC assays, *N. benthamiana* leaf epidermis (abaxial side) was examined after transient plasmid transformation using the same confocal system (excitation: 488 nm for YFP, 555 nm for mRFP; detection: 500–580 nm for YFP, 570–650 nm for mRFP). Images were processed using Zen and ImageJ softwares.

Yeast two-hybrid assay

The yeast two-hybrid assay followed Paiano et al. (2019), using the *pJ696* yeast strain (Lafuente et al. 2000) and nlsGFP as a negative control.

Electrophoretic mobility shift assay (EMSA)

Recombinant proteins were expressed in *E. coli* BL21(DE3) cells, which were transformed with expression vectors. Cultures were grown at 30 °C to OD600 0.3–0.5, then induced with 0.5 mM isopropyl β-D-1-thiogalactopyranoside (IPTG) for 5 h. Cells were harvested by centrifugation, frozen, and lysed in a buffer (50 mM Tris–HCl, pH 8, 500 mM NaCl, 30 mM imidazole, 0.5 mM DTT, 1 mM PMSF, lysozyme, and protease inhibitors) by sonication. The lysate was clarified by centrifugation, and the protein was purified using an Ni–NTA column. After washing, proteins were eluted with 300 mM imidazole. Protein concentration was measured using a Qubit fluorometer. For the EMSA assay, complementary oligonucleotides encoding the MEME motif were synthesized, with one oligo tagged with Cyanine3 (Table S1). Equimolar concentrations (10 µM) of oligos were mixed in STE buffer (100 mM NaCl, 10 mM Tris–HCl, pH 8, 1 mM EDTA) and annealed using a PCR thermocycler with the following program: 98 °C for 3 min, 75 °C for 1 h, 65 °C for 1 h, 37 °C for 30 min, and 25 °C for 10 min. For binding assays, the double-stranded DNA substrate (1 nM) was incubated with the purified protein in a binding buffer containing 25 mM Tris–HCl (pH 7.5), 9% glycerol, 75 mM NaCl, 5 mM DTT, 5 mM $MgCl_2$, and 1 mg/mL BSA at room temperature for 20 min. For negative controls without proteins, SEC buffer (50 mM Tris–HCl, pH 8, 10% glycerol, 50 mM NaCl and 5 mM Na_2EDTA) was used. The reaction was separated on a 10% polyacrylamide gel and visualized using a Typhoon scanner (Cytiva).

Dual luciferase assay

Agrobacterium strains containing the reporter control plasmid (*p35S::REN*), the promoter reporter plasmid (*promoter::LUC*) and the protein expression plasmid (*pUBQ::TranscriptionFactor* or *p35S::TranscriptionFactor*) were infiltrated together in *N. tabacum* leaves. A green

fluorescent protein (GFP) fused to a nuclear localization signal (nls) was used as negative control for the protein expression plasmid. Three days later, 5 mg of leaf tissue was harvested, snap-frozen and stored at − 80 °C. Samples were grinded in a tissue-grinder (Retsch, MM400) three times at 30 Hz for 30 s. Then, samples were resuspended in 100 µL of passive lysis buffer 1X (PLB) from the dual luciferase reporter assay system kit (Promega, E1910) and washed by centrifugation (7500 *g*, 1 min, RT). The supernatant was transferred into a new 1.5 mL Eppendorf tube and centrifugated again (7500 *g*, 1 min, RT). A total of 40 µL of supernatant was mixed with 60 µL of passive lysis buffer 1X (PLB) to obtain a 100µL lysate. The dual luciferase activity measurement was made following the manufacturer's standard protocol (Promega, E1910), using a Sirius L tube luminometer (Titertek-Berthold, 110 401 10).

Results

Ectopic induction of AmMIXTA unravels genes integral to long-stalked glandular trichome development

In this study, we investigated the transcriptional cascade triggered by *AmMIXTA* heterologous expression leading to the induction of supernumerary long-stalked glandular trichomes in *N. tabacum* (Glover et al. 1998; Payne et al. 1999; Perez-Rodriguez et al. 2005). Induction of short-stalked glandular or non-glandular trichome development was not observed. Driving *AmMIXTA* expression with a *β*-estradiol inducible promoter (Curtis and Grossniklaus 2003), we aimed to dissect the molecular mechanisms governing long-stalked glandular trichome initiation and development on the cotyledons of tobacco.

Expression of *AmMIXTA* resulted in a pronounced trichome-rich phenotype on the cotyledons and hypocotyl, as evidenced by comparative analysis of induced and non-induced plants (Fig. 1a-e and Fig. S1a, b). Microscopic examination revealed an increase in long-stalked glandular trichome density from 1.67 ± 5.34 to 664.33 ± 346.58 cm^{-2} upon *AmMIXTA* induction (Fig. 1e), confirming its role in redirecting protodermal cell fate towards trichome formation (Glover et al. 1998; Payne et al. 1999; Perez-Rodriguez et al. 2005). Ectopically induced long-stalked trichomes exhibited a morphology similar to naturally occurring ones, with chlorophyll autofluorescence indicating the presence of chloroplasts in glandular cells (Fig. S1c–e). In addition, rhodamine B staining, a dye used for acylsugar labeling, marked the trichome heads, suggesting secondary metabolite biosynthesis activities in the gland (Fig. S1e). Nuclear localization of AmMIXTA was confirmed using a VENUS-tagged version of the protein (Fig. S1f).

Using the *AmMIXTA* inducible system, we conducted RNA-seq to identify genes crucial for initiating and driving the development of long-stalked glandular trichomes. Seedlings treated with 10 µM *β*-estradiol for 4 h and 48 h were compared to non-induced controls (Fig. S2). RT-qPCR validation confirmed significant upregulation of *AmMIXTA* transcripts, by 37-fold at 4 h and 138-fold at 48 h (Fig. 2a), with trichome formation observed prominently at 48 h. Subsequent RNA-seq analysis yielded a high-quality mapping to the *N. tabacum* genome (Sierro et al. 2014) (Table S2), identifying 719 and 1947 DEGs at the 4 and 48 h time points ($0.67 >$ Fold change and Fold change > 1.5, $P < 0.05$) (Table S4a and b). Emphasis was placed on analyzing upregulated genes in subsequent data analyses due to this cell fate reprogramming. Among these, 166 and 604 genes were upregulated at 4 h and 48 h, respectively, with some genes upregulated at both time points (Fold change > 1.5, $P < 0.05$) (Fig. 2b and Table S4a). The 4 h post-*AmMIXTA* induction captures genes involved in early stages of long-stalked glandular trichome development, while 48 h post-induction captures cell trans-differentiation into glandular trichome cells. In total, five genes, all transcription factors, were upregulated at both time points: two bHLHs, one AP2/ERF, one TRIHELIX transcription factor and one protein containing a MYB domain (Fig. 2b, c).

GO term enrichment analysis via PANTHER ($P < 0.05$) illustrates distinct biological function enrichment patterns of upregulated DEGs at 4 and 48 h post-*AmMIXTA* induction, reflecting the dynamic nature of trichome development (Fig. 2d, e; Fig. S3, Table S5) (Mi et al. 2019; Thomas et al. 2022). At 4 h post-induction, enrichment included terms associated among others with developmental processes and responses to stimuli (Fig. 2d, Table S5), and at 48 h with developmental processes (Fig. 2e, Table S5) and secondary metabolite biosynthesis (including isoprenoid metabolic process). The observed enrichments align with expected GO categories for glandular trichome development and differentiation. This broad transcriptional response aligns with findings from other plant species, reinforcing the idea that trichome development is governed by a conserved pathway intersecting with stress responses (Plett et al. 2010; Gao et al. 2021; Wang et al. 2021).

Our GO term analysis, matching those from other trichome studies, suggests a similar genetic framework across species. For example, in *Populus trichocarpa*, *Pta-MYB186* overexpression, an *AmMIXTA* ortholog, increased trichome production and enrichment of GO terms associated with defense, cell division, photosynthesis, cell wall composition, and hormonal regulation (Plett et al. 2010). In *Capsicum annum*, differences in gene expression between hairless and hairy plants involved hormonal signal transduction and resistance (Gao et al. 2021).

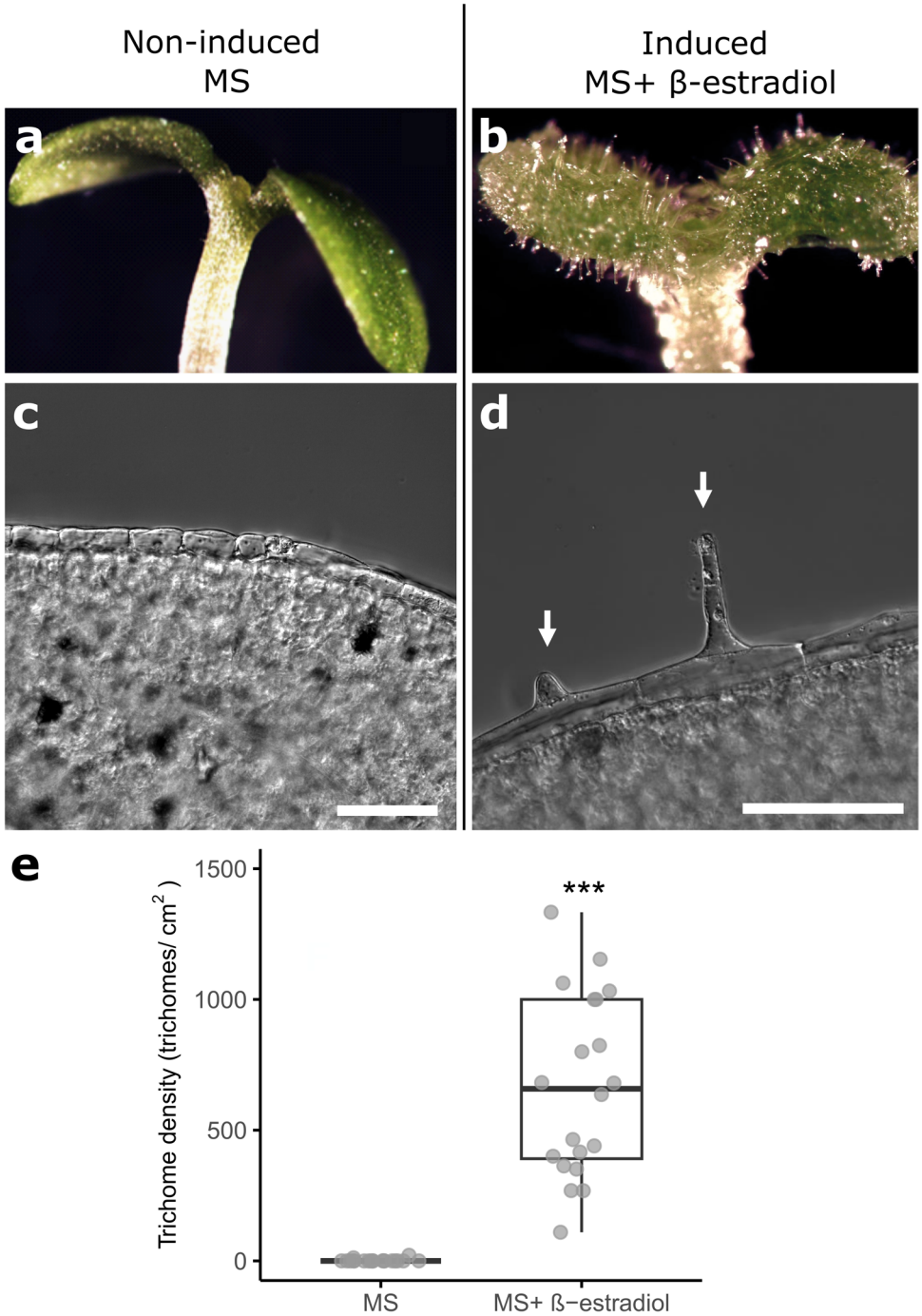

Fig. 1 Phenotype of *pEST::AmMIXTA* transgenic plants. **a**–**d** Ten-day-old *pEST::AmMIXTA* seedlings germinated on non-inducing medium (1⁄2 MS medium) (**a**, **c**) and inducing medium (1/2 MS medium supplemented with 10 µM *β*-estradiol) (**b**, **d**). Differential Interference Contrast (DIC) pictures of the epidermal layer. Arrows indicate developing trichomes. Scale bar represents 100 µm. **e** Trichome density on induced and non-induced seedlings presented as a boxplot ($n = 20$ plants). Individual data points are depicted as dots. Asterisks denote significant differences from the MS condition as determined by Student's t-test: $***P < 0.001$

In *NtCYCB2*-overexpressing and downregulating lines, DEGs were linked to secondary metabolite biosynthesis, stress resistance and transport mechanisms (Wang et al. 2021). Trichomes aid in defense against biotic and abiotic stresses, regulated by internal signals like phytohormones and external stimuli; hence the stress-related GO terms were prominently identified (Hauser 2014). Similar GO terms enrichment was observed in *Arabidopsis* trichome and leaf transcriptomes (Jakoby et al. 2008).

Transcription factors involved in long-stalked glandular trichome initiation and development

Further dissecting the dataset, we cross-referenced the upregulated genes at both time points with genes referenced as transcription factor in the Plant TFBD (Jin et al. 2017) database and on PANTHER (Thomas et al. 2022). This yielded two distinct lists: one comprising 15 transcription factors at 4 h, likely involved in the initiation of long-stalked glandular trichome development, and another

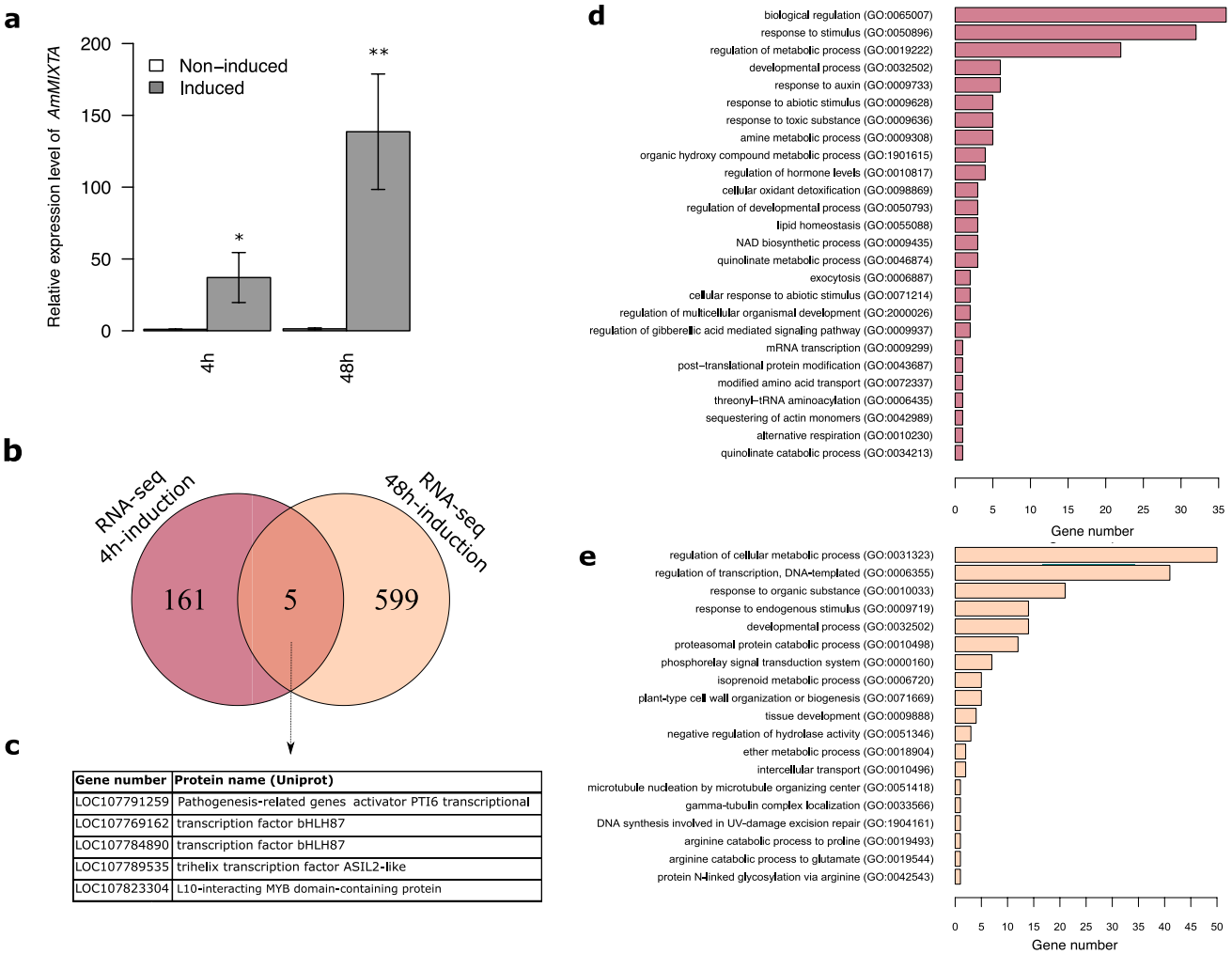

Gene number	Protein name (Uniprot)
LOC107791259	Pathogenesis-related genes activator PTI6 transcriptional
LOC107769162	transcription factor bHLH87
LOC107784890	transcription factor bHLH87
LOC107789535	trihelix transcription factor ASIL2-like
LOC107823304	L10-interacting MYB domain-containing protein

Fig. 2 RNA-seq analysis 4 h and 48 h after β-estradiol induction of *pEST::AmMIXTA*. **a** Expression level of *AmMIXTA* in 10-day-old seedlings germinated on 1/2 MS medium and subjected to β-estradiol induction for 4 h and 48 h compared to the control in non-inducible conditions (1/2 MS). Expression normalization was performed using the geometric averaging of multiple housekeeping genes (*NtEF2*, *NtACTIN*, *NtUBC2*). Values represent means ± SE, $n = 3$. Asterisks denote significant differences compared to non-induced conditions as determined by Student's t test: $*P < 0.05$; $**P < 0.001$. **b** Differentially up-regulated genes between the *pEST::AmMIXTA* seedlings induced with β-estradiol for 4 h and 48 h, and their own non-induced controls, represented by a Venn diagram. **c** List of the genes differentially up-regulated genes at 4 and 48 h. **d**, **e** GO functional enrichment analysis based on the differentially up-regulated genes at 4 h (**d**) and 48 h (**e**). The graphs represent categories with a statistically significant difference between induced and non-induced plants ($P < 0.05$). The x-axis represents the fold enrichment of genes observed in the RNA-seq data over the expected number in the reference list. The y-axis shows the over-represented GO terms from the Biological Process classification according to PANTHER

consisting of 32 candidates at 48 h, associated with further development and differentiation (Table 1).

Both lists featured key transcription factor families known for their role in trichome development in Solanaceae, including bHLHs, C2H2 zinc-finger proteins, MYBs, HD-ZIPs and WRKYs. This approach highlighted the transcription factors critical for both the onset and progression of long-stalked glandular trichome development, illustrating the complexity of the regulatory network involved.

NtZFP8 is expressed in developing trichomes

Various C2H2 zinc finger protein transcription factors, including AtZFP6, AtGIS, AtGIS3, NbGIS, JcZFP8, SlHAIR and SlHAIR2, play significant roles in trichome formation in *Arabidopsis*, tomato, and tobacco (Gan et al. 2007; Zhou et al. 2013; Sun et al. 2015; Liu et al. 2018; Shi et al. 2018; Zheng et al. 2021).

Through our analysis, *ZINC FINGER PROTEIN 8* (*NtZFP8*; LOC107828820), emerged as coding for a

Table 1 Transcription factors induced at 4 h and/or 48 h post-induction of *AmMIXTA*

	Gene number	Gene annotation (Panther)	Protein name (Uniprot)
4 and 48 h	LOC107791259	AP2/ERF domain-containing protein	PTI6-like
	LOC107769162	BHLH domain-containing protein	bHLH87-like
	LOC107784890	BHLH domain-containing protein	bHLH87-like
	LOC107789535	trihelix transcription factor ASIL2-like	ASIL2-like
4 h	LOC107795711	Protein NLP7-like	NLP1-like
	LOC107809138	NAC domain-containing protein	NAC073-like
	LOC107782024	AP2/ERF domain-containing protein	PTI6-like
	LOC107822913	transcription factor bHLH87-like	bHLH87-like
	LOC107817147	BHLH domain-containing protein	bHLH66-like/LRL1
	LOC107809542	Dof zinc finger protein DOF2.1-like	DOF2.1-like
	LOC107777300	BZIP domain-containing protein	bZIP61-like
	LOC107828820	C2H2-type domain-containing protein	ZFP8-like
	LOC107807804	BHLH domain-containing protein	bHLH96-like
	LOC107817904	Transcription factor HEC1-like	HEC1-like
	LOC107803280	Squamosa promoter-binding-like protein 16	SPL16-like
	LOC107759491	PPC domain-containing protein	AHL28-lik2
	LOC107763608	Transcription repressor KAN1-like	KAN1-like
	LOC107795152	Homeobox domain-containing protein	HAT4-like
	LOC107817975	HTH myb-type domain-containing protein	GLK1-like

Table 1 (continued)

	Gene number	Gene annotation (Panther)	Protein name (Uniprot)
48 h	LOC107785557	NAC transcription factor 56-like	NAC56-like
	LOC107818808	Homeobox domain-containing protein	ATHB12-like
	LOC107772091	Homeobox domain-containing protein	ATHB-12-like
	LOC107765920	Homeobox domain-containing protein	ATHB12-like
	LOC107830350	Transcription factor UNE10-like	UNE10-like
	LOC107802018	NAC domain-containing protein 7-like	NAC7-like
	LOC107771009	NAC domain-containing protein 72-like	NAC72-like
	LOC107769826	HSF_DOMAIN domain-containing protein	HSFB2B-like
	LOC107777523	WRKY domain-containing protein	WRKY23-like
	LOC107769162	Transcription factor bHLH87-like	bHLH87-like
	LOC107799348	LOB domain-containing protein 40-like	LOB40-like
	LOC107821658	AP2/ERF domain-containing protein	TINY-like
	LOC107823244	HSF_DOMAIN domain-containing protein	HSFB2B-like
	LOC107817617	Squamosa promoter-binding-like protein 9	SPL16-like
	LOC107811176	LOB domain-containing protein 41-like	LOB41-like
	LOC107801705	LOB domain-containing protein 1-like	LOB1-like
	LOC107828406	Protein SENSITIVE TO PROTON RHIZOTOXICITY 1-like	STOP1-like
	LOC107765862	NAC domain-containing protein 72-like	NAC72-like
	LOC107818886	BZIP domain-containing protein	bZIP53-like
	LOC107794837	HSF_DOMAIN domain-containing protein	HSFA7a-like
	LOC107793383	DDT domain-containing protein	RLT3-like
	LOC107775044	HSF_DOMAIN domain-containing protein	HSFA2b-like
	LOC107806678	GATA transcription factor 15-like	GATA15-like
	LOC107785821	BZIP domain-containing protein	bZIP17-like
	LOC107805484	myb-related protein 330-like	MYB330-like
	LOC107791263	GRAS domain-containing protein	SCL30-like
	LOC107770678	AP2/ERF domain-containing protein	CRF4-like
	LOC107806890	BZIP domain-containing protein	GBF4-like
	LOC107827724	Protein REVEILLE 3-like	RVE3-like
	LOC107764381	transcription factor EGL1-like	EGL1-like
	LOC107789254	GRF1-interacting factor 3-like	GRF1-like
	LOC107827709	GATA transcription factor 5-like	GATA5-like

noteworthy ZFP transcription factor, exhibiting significant upregulation 4 h following the induction of *AmMIXTA*. NtZFP8 is the closest homolog of AtZFP8 in *Arabidopsis thaliana* (Fig. S4a and b). To understand its role in trichome development in *N. tabacum*, we examined its expression across various tissues. RT-qPCR results showed that *NtZFP8* expression is higher in developing leaves than in mature leaves, suggesting a role during trichome initiation and development (Fig. 3a). This was further confirmed using a *NtZFP8* promoter reporter line (*pNtZFP8:nlsGFP-GUS*), which demonstrated promoter activity localized to the epidermal layer during early developmental stages (Fig. 3b). In leaf primordia, *NtZFP8* promoter activity was observed in epidermal pavement cells, stomata, non-glandular trichomes, long-stalked glandular trichomes (stalk and developing glandular heads at 1–2 cell stages), and short-stalked glandular

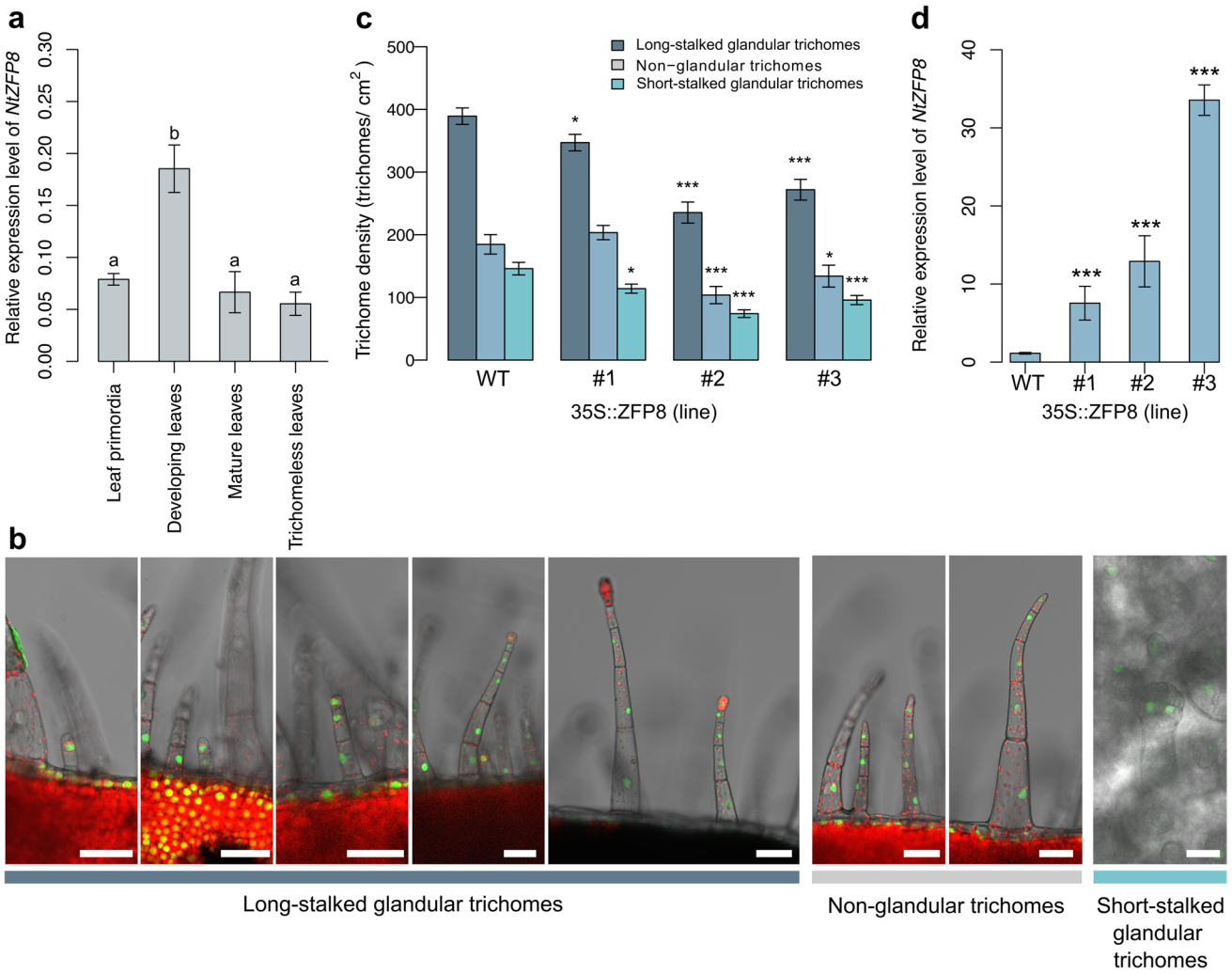

Fig. 3 *NtZFP8* expression pattern in leaves. **a** RT-qPCR analysis of different tissues (leaf primordia, developing leaves, mature leaves, and leaves without trichomes) from WT plants. Gene expression levels are expressed relative to the geometric mean of three different internal controls (*NtEF2, NtACTIN, NtUBC2*). Results are displayed as mean ± SE, $n = 4$. Significant differences were determined by ANOVA, with each letter indicating a significant variation between tissues ($P < 0.05$). **b** Reporter lines *pZFP8::nlsGFP-GUS* showing expression in different types of trichomes during their development in expanding leaves of 6-week-old plants. Scale bars represent 50 µm; green indicates nlsGFP; red denotes chlorophyll autofluorescence. **c** Trichome density in different independent lines *p35S::ZFP8*. **d** Expression level of *NtZFP8* in the overexpressing lines measured by RT-qPCR. Gene expression levels are expressed relative to the WT and the geometric mean of three different internal controls (*NtEF2, NtACTIN, NtUBC2*). Asterisks denote significant differences to WT as determined by Student's t test: ***$P < 0.001$, **$P < 0.01$ and *$P < 0.05$

trichomes (stalk and head). This expression is consistently present in developing trichomes but ceases post-development. In mature leaves, *NtZFP8* expression is no longer detectable in trichomes but remains active in some epidermal pavement cells and stomata (Fig. S5).

In *NtZFP8* overexpressing lines (*p35S::NtZFP8*), the density of all three trichome types in fully grown leaves was generally significantly reduced compared to wild type (WT) plants (Fig. 3c, d). Trichomes did not present any morphological defect or developmental alteration, only a change in density. This phenotype suggests that NtZFP8 would influence trichome development in *N. tabacum*.

Convergent transcriptional targets of *AmMIXTA* and NtZFP8 in tobacco

We investigated a potential physical interaction between AmMIXTA and NtZFP8 using a yeast-2-hybrid assay (Paiano et al. 2019). *AmMIXTA* coding sequence (CDS) was fused to the GAL4 activation domain (AD), and *NtZFP8* CDS to the GAL4 binding domain (BD). Colonies containing AD-AmMIXTA and BD-NtZFP8 grew in a similar way on SD-WL (selective medium without tryptophan and leucine). A significant growth differences on SD-HAWL (medium without histidine and adenine) was observed and

indicated a physical interaction between AmMIXTA and NtZFP8 (Fig. 4a).

The interaction between AmMIXTA and NtZFP8 was further validated using Bimolecular Fluorescence Complementation (BiFC). When AmMIXTA was fused to the C-terminal fragment of YFP and co-expressed with NtZFP8 fused to the N-terminal fragment of YFP, the reconstituted YFP fluorescence signal confirmed their interaction (Fig. 4b) (Grefen and Blatt 2012).

To unravel the downstream pathways regulated by AmMIXTA and NtZFP8 and so identify the transcriptional targets of both transcription factors, we employed DNA affinity purification sequencing (DAP-seq) (Bartlett et al. 2017). DNA sequences that were bound to the transcription factors were sequenced and mapped to the *N. tabacum* genome (Sierro et al. 2014) (Table S3). Hits were identified by comparing against the negative control (nlsGFP protein), (peak shape score < 2 and $P < 0.05$) to delineate significant binding regions.

Among all the regions significantly enriched in the analysis, 6.4% (1874 hits) for AmMIXTA and 5.8% (1235 hits) for NtZFP8 were in regions surrounding annotated genes (− 3 and 1 kb, respectively, before the start codon and after the stop) corresponding respectively to 1162 and 974 distinct genes. The rest were in intergenic regions and not further included in the subsequent analysis (Table S6 and S7). Among the genes of interest, 425 genes targeted by AmMIXTA and 265 by NtZFP8 were annotated as uncharacterized. Analysis of the binding site locations surrounding annotated genes revealed that, for both AmMIXTA and NtZFP8, a significant majority (over 80%) of the interactions were localized to regions upstream of the START codon, encompassing promoter regions and 5' untranslated regions (UTRs), as well as within introns (Fig. 5a, b).

Utilizing the MEME suite for motif discovery (Bailey et al. 2015), we identified specific DNA sequences preferentially bound by each transcription factor: AmMIXTA showed a strong affinity for the GGTGGTGGTGG motif, with an *e*-value of 2.2×10^{-902} (Fig. 5c), whereas NtZFP8 predominantly bound to the TBCTTYTYCTTCTTY motif, with an e-value of 2.6×10^{-76} (Fig. 5d). Motif binding sites were confirmed using electrophoretic mobility shift assay (EMSA) confirming a binding to CTTCTTCTTCT for NtZFP8 and to GGTGGTGGTGG for AmMIXTA, a motif similar to the GGTAGGT motif already identified for several MYB proteins (JASPAR database) (Rauluseviciute et al. 2024) (Fig. 5c, d).

When examining the overlap in genes targeted by both transcription factors, we identified 752 common genes, representing 45 and 77% of the total number of genes targeted by AmMIXTA and NtZFP8, respectively (Fig. 5e). Notably, the top 15 shared targets of both proteins

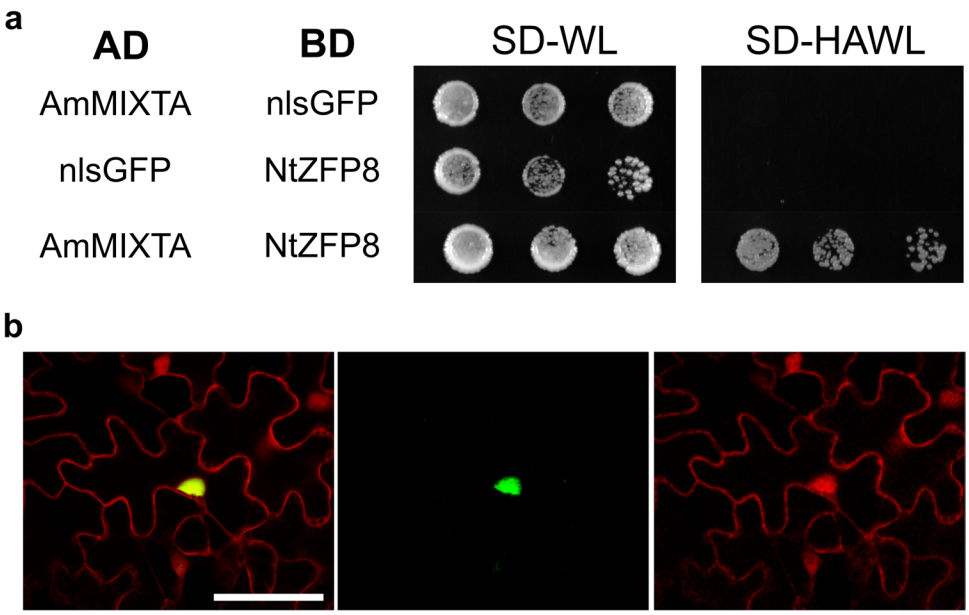

Fig. 4 Interaction of NtZFP8 with AmMIXTA. **a** Yeast two-hybrid assay was performed using a control medium lacking tryptophan and leucine (SD/-WL) and a selective medium devoid of tryptophan, leucine, histidine, and adenine (SD/-HAWL) to investigate the interaction between AmMIXTA and NtZFP8. nlsGFP served as the negative control for the interaction. 'AD' represents the activation domain 'BD' the binding domain and 'SD' refers to synthetically defined medium. The experiment was replicated three times, consistently showing similar results. **b** Bimolecular Fluorescence Complementation (BiFC) was carried out by fusing AmMIXTA to the C-terminal fragment of YFP and NtZFP8 to the N-terminal fragment of YFP. The reconstituted YFP fluorescence signal confirmed their physical interaction. Left panel, YFP and mRFP signal; middle panel, YFP alone; right panel, mRFP alone. Scale bar represents 50 µm

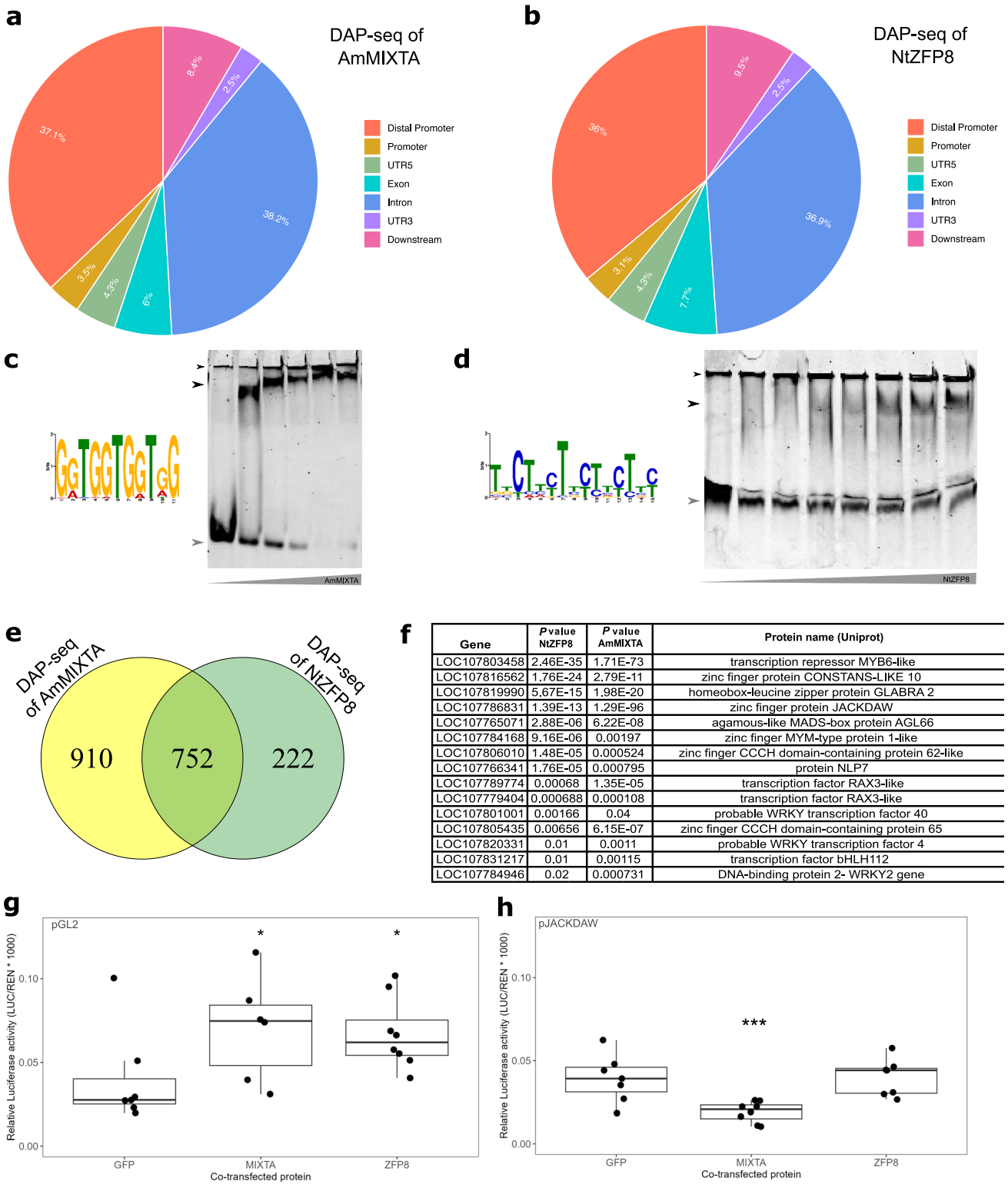

f

Gene	*P* value NtZFP8	*P* value AmMIXTA	Protein name (Uniprot)
LOC107803458	2.46E-35	1.71E-73	transcription repressor MYB6-like
LOC107816562	1.76E-24	2.79E-11	zinc finger protein CONSTANS-LIKE 10
LOC107819990	5.67E-15	1.98E-20	homeobox-leucine zipper protein GLABRA 2
LOC107786831	1.39E-13	1.29E-96	zinc finger protein JACKDAW
LOC107765071	2.88E-06	6.22E-08	agamous-like MADS-box protein AGL66
LOC107784168	9.16E-06	0.00197	zinc finger MYM-type protein 1-like
LOC107806010	1.48E-05	0.000524	zinc finger CCCH domain-containing protein 62-like
LOC107766341	1.76E-05	0.000795	protein NLP7
LOC107789774	0.00068	1.35E-05	transcription factor RAX3-like
LOC107779404	0.000688	0.000108	transcription factor RAX3-like
LOC107801001	0.00166	0.04	probable WRKY transcription factor 40
LOC107805435	0.00656	6.15E-07	zinc finger CCCH domain-containing protein 65
LOC107820331	0.01	0.0011	probable WRKY transcription factor 4
LOC107831217	0.01	0.00115	transcription factor bHLH112
LOC107784946	0.02	0.000731	DNA-binding protein 2- WRKY2 gene

primarily binding in regions upstream of the START codon, mainly comprised genes encoding key transcription factor families such as MYBs, zinc fingers, bHLHs, HD-ZIPs, and WRKYs, indicating a focused regulatory impact on the essential components of the plant transcriptional machinery known to impact epidermal patterning, (Fig. 5f and Fig. S6).

Since *AtGL2,* the closest homolog of *NtGL2* in *Arabidopsis* (Fig. S4c and d), and *CsGL2* are known to promote trichome formation (Rerie et al. 1994; Cui et al. 2016),

◂**Fig. 5** Direct DNA targets of AmMIXTA and NtZFP8 transcription factors. **a**, **b** Distribution of AmMIXTA-binding peaks relative to gene structures (**a**) and NtZFP8-binding peaks (**b**). Definitions for gene regions: distal promoter (from − 3 kb to − 0.5 kb before the START codon); Promoter (from − 0.5 kb up to the 5′ UTR); UTR5: 5′ untranslated region, UTR3: 3' untranslated region, exon, intron and downstream region (from the end of the 3′ UTR to 1 kb after the STOP codon). **c** The top-scoring motif, GGTGGTGGTGG, was identified with an *e*-value of $2.2\times10-902$, according to MEME analysis. Gel-shift assay shows a binding of AmMIXTA to the fluorescent DNA substrate: GGTGGTGGTGG; protein concentrations were used from 0 to 3000 nM. **d** The top-scoring motif, TBCTTYTYCTTCTTY was identified with an *e*-value of $2.6\times10-76$ according to MEME analysis. Gel-shift assay shows a binding of NtZFP8 to the fluorescent DNA substrate: CTTCTTCTTCT; protein concentrations were used from 0 to 4400 nM. Black arrow head, bound DNA; gray arrow head, unbound DNA; small black arrow, wells. **e** Venn diagram showing the overlap between AmMIXTA and NtZFP8 targets. **f** Identification of the top 15 transcription factors shared by AmMIXTA and NtZFP8, as revealed through the DAP-seq assay. **g-h** Dual luciferase assay to test the binding of AmMIXTA and NtZFP8 on *pGL2* (**g**) and *pJACKDAW* (**h**) promoters. Asterisks denote significant differences to WT as determined by Student's t test: $***P<0.001$, $**P<0.01$ and $*P<0.05$

we examined the expression pattern of the gene coding for the homeobox–leucine zipper protein *GLABRA 2,* (*NtGL2,* LOC107819990), using a reporter construct (*pNtGL2::nlsGFP-GUS*, Fig. S7a). *NtGL2* promoter activity was detected in the stalks of developing long-stalked glandular and non-glandular trichomes. We also investigated the gene coding for the zinc finger protein *JACKDAW* (*NtJACKDAW*, LOC107786831), a gene of particular interest because its closest ortholog in *Arabidopsis*, *AtJACKDAW* (Fig. S4e and f), plays a crucial role in the spatial regulation of *AtGL2* expression, thereby ensuring proper root hair patterning (Hassan et al. 2010). Interestingly, the *NtJACKDAW* promoter (*pNtJACKDAW::nlsGFP-GUS*) displayed a trichome expression pattern similar to that of the *NtGL2* promoter (Fig. S7b). Dual–luciferase assays further demonstrated that AmMIXTA negatively regulates *NtGL2* promoter activity, whereas both AmMIXTA and NtZFP8 positively regulate *NtJACKDAW* promoter activity (Fig. 5g–h).

Discussion

Our research exploited ectopic expression of *AmMIXTA*, acting as a transcriptional switch inducing long-stalked glandular trichome formation to elucidate the transcriptional cascade leading to the development of those trichomes in *N. tabacum*. Results confirmed AmMIXTA as a master regulator orchestrating a complex developmental cascade, specifically inducing long-stalked glandular trichomes in cotyledon epidermal cells without affecting other cell types (Fig. 1, 2a and Fig. S1) (Glover et al. 1998; Payne et al. 1999). This suggests the presence of an endogenous MIXTA-like homolog in tobacco, likely regulating glandular trichome development through a transcriptional network similar to the one described in this study.

Transcription factors at the crossroads of trichome initiation and development

Leveraging RNA-seq analysis at critical post-induction intervals (4 and 48 h) allowed us to capture the dynamic nature of the transcriptional response elicited by AmMIXTA. Focusing on upregulated genes, the significant increase in DEGs from 166 at 4 h to 604 at 48 h not only illustrates the expanding regulatory influence of AmMIXTA over time but also suggests a phased activation of the downstream transcriptional network (Fig. 2a–c and Fig. S2).

Importantly, *AmMIXTA* induction altered the density but not the morphology of long-stalked glandular trichomes. This indicates that *AmMIXTA* acts primarily at the initiation stage of this trichome type, whereas subsequent differentiation likely requires additional endogenous regulators. Supporting this view, most known trichome regulators showed no significant expression changes at 4 h post-induction (Fig. S8a), consistent with early initiation being *AmMIXTA*-dependent. By 48 h, corresponding to differentiation/maturation stages, we observed upregulation of *NtMYC1* and *NtSPL9* and downregulation of regulators including *NtMYBML1*, *NtWOOLLY*, *NtHD1*, *NtHD9*, *NtHD13*, and *NtMYB1* (Fig. S8a). These later changes likely reflect broader transcriptomic reprogramming associated with trichome proliferation.

Our research examines transcriptional regulation of trichome development, focusing on transcription factors known for their roles in trichome development across various plant species (Table 1). Although a role in cuticle and cell wall formation can be hypothesized for AmMIXTA as is the case of its AaMIXTA homolog (Noda et al. 1994; Shi et al. 2017), several of the identified transcription factors or their close homologs have already been associated with trichome development in previous studies. Interestingly, the overexpression of *AmMIXTA* reduces the expression level of one of its closest homolog in *N. tabacum*, *NtMYB16-like* (LOC107791424), suggesting that *AmMIXTA* could be redundant to this MYB gene (Fig. S8b).

MYB transcription factors, including AtMYB106 and AtGL1, are essential for trichome initiation and development (Han et al. 2022). We identified the transcription activator GOLDEN2-like protein (NtGLK1, LOC107817975) and the transcriptional repressor KANADI (NtKAN1, LOC107763608) at the trichome initiation stage (4 h post-induction). In *Arabidopsis*, GOLDEN2-like proteins support cellular differentiation (Chen et al. 2016), while AtKAN1 regulates trichome development by interacting with AtGL1 (Wang et al. 2019). HD-ZIP IV members, such

as SlWOOLLY and AtGL2, and HD-ZIP I members, like CsGL1, TINY BRANCHED HAIR (CsTBH), and MICRO-TRICHOME (CsMICT), are crucial for trichome morphogenesis (Han et al. 2022; Wu et al. 2023, 2024a, b; Khosla et al. 2014). Our study identified homeobox–leucine zipper proteins from the HD-ZIP I sub-family (NtATHB12; LOC107818808, LOC107765920, LOC107772091) as potential contributors to trichome development. Our RNA-seq analysis also revealed several genes coding for bZIP factors potentially influencing trichome development in *N. tabacum*, including *b-ZIP TRANSCRIPTION FACTOR 53-like* (*NtbZIP53*; LOC107818886), which is connected to jasmonate responses in *Arabidopsis* (Wu et al. 2024b). The importance of bHLH transcription factors in trichome development is well documented: AtGL3, AtEGL3 (Payne et al. 2000; Zhang et al. 2003) and SlbHLH95 (Chen et al. 2020). Here, we identified the gene coding for the transcription factor EGL1 (NtEGL1; LOC107764381) as upregulated after 48 h. Its closest *Arabidopsis* ortholog is AtGL3, a well-characterized regulator of trichome development. Another bHLH gene coding for a transcription factor bHLH066-like *bHLH066-likebHLH066-likebHLH066-like* (NtbHLH066-like; LOC107817147) was upregulated at 4 h. It is closely related to AtbHLH066/Lj-RHL1-LIKE1 (AtLRL1), a gene linked to root hair elongation and branching. In *Arabidopsis*, AtLRL1 function is suppressed by AtGL2 in non-hair cells, suggesting a possible role in trichome development (Bruex et al. 2012; Lin et al. 2015). (Khosla et al. 2014).

WRKY transcription factors, such as the probable WRKY transcription factor 23 (NtWRKY23, LOC107777523), may also play roles in trichome development and differentiation (Ishida et al. 2007; Grunewald et al. 2012; Xie et al. 2021). C2H2-type zinc finger proteins are important in developmental processes and stress responses (Chang et al. 2018; Liu et al. 2018; Gao et al. 2021; Zheng et al. 2021), regulating trichome development through hormonal pathways (Liu et al. 2018). In our study, *NtZFP8* was significantly upregulated at 4 h, suggesting its involvement in trichome development.

In the current model describing the transcriptional network regulating glandular trichome development in *S. lycopersicum*, SlWOOLLY is needed to control the balance between peltate and digitate trichome development via SlMX1, among others (Wu et al. 2024a). Here, *NtWOOLLY* was not found to be induced by the overexpression of *AmMIXTA*, suggesting that AmMIXTA could be acting downstream or even independently from this latter. In our case *AmMIXTA* is sufficient to induce long-stalked glandular trichome formation without impacting non-glandular and short-stalked trichome development. This could be related to the activity of SlMX1, AmMIXTA closest homolog in tomato (Wu et al. 2024a). SlMX1 has been shown to work alongside SlWOX3 to increase the number of digitate trichomes while reducing the number of peltate trichomes (Ewas et al. 2016).

Regulation of trichome development by NtZFP8 and its interaction with AmMIXTA

NtZFP8 is a close ortholog of the uncharacterized *SlZFP8* (*Solyc03g058160*) in tomato, whose role in glandular trichome development remains unknown (Fig. S9). In contrast, SlHAIR(*Solyc10g078970*) and SlZFP8L/SlHAIR2 (*Solyc10g078990*), paralogs of SlZFP8 (Fig. S9), are well-characterized C2H2 zinc finger proteins that directly interact with SlWOOLLY to regulate trichome initiation and elongation via SlZFP6 (Chang et al. 2018; Zheng et al. 2021). It was observed that *NtZFP8* is expressed in all types of developing trichomes and in the epidermis suggesting a potential role in their initiation and/or their development (Fig. 3a, b). However, the activity of the *NtZFP8* promoter was not restricted to trichomes but also detected in the epidermis and stomata. This suggests that the functional specificity of NtZFP8 in trichome development may rely on post-transcriptional regulation or protein–protein interactions that restrict its activity to trichomes. Such specificity could be achieved through the presence of trichome-specific co-factors or partners required for NtZFP8 function. This is consistent with growing evidence that transcription factor specificity in plant epidermal patterning is often conferred through combinatorial interactions rather than promoter exclusivity as already observed in the context of trichome development (Wu et al. 2023). To further investigate the role of NtZFP8 in trichome development, transgenic lines overexpressing *NtZFP8* were generated (Fig. 3b). In *p35S::NtZFP8* lines, a significant decrease in trichome density—including both glandular and non-glandular types—was observed (Fig. 3c, d). This finding suggests that NtZFP8 might function as a putative repressor of trichome development, playing a potential antagonistic role to MIXTA-like transcription factor. Given the contrasting phenotypes of *NtZFP8* and *AmMIXTA* overexpression lines, it could be possible that *NtZFP8* is induced in *MIXTA*-induced transgenic lines, where it could modulate AmMIXTA transcriptional activity as part of a negative feedback mechanism to fine-tune trichome development in these lines (Wu et al. 2023).

Alternatively, the potential inhibitory effect of *NtZFP8* overexpression observed in *p35S::NtZFP8* lines on trichome development could result from an artificial titration effect, in which NtZFP8 binds and sequesters an endogenous MIXTA-like partner with trichome-promoting activity, acting as a dominant-negative allele, rather than reflecting its normal regulatory function. Further functional validation including loss-of-function analysis will be necessary to definitively confirm the role of *NtZFP8* in trichome development.

To date, evidence for zinc finger proteins acting as negative regulators of trichome development remains limited (Han et al. 2021). While in tomato, SlHAIR2 is considered as a positive regulator of trichome development (Zheng et al. 2021), its mutant exhibits an intermediate phenotype, with a reduction in type I and II trichomes but an increase in types III and IV, suggesting that SlHAIR2 may promote the formation of certain trichome types while repressing the development of others (Gasparini et al. 2023). In root hair development, a process sharing common genes with trichome development (Ishida et al. 2008), AtZP1 was identified as a zinc finger protein that negatively regulates root hair development and is transcriptionally controlled by AtGL2 (Han et al. 2020). Further research is therefore needed to clarify the precise mode of action of NtZFP8 in *planta*.

Interestingly, the interaction between AmMIXTA and NtZFP8 was confirmed by yeast two-hybrid assays and Bimolecular Fluorescence Complementation (BiFC) (Fig. 4a, b). This interaction suggests a possible regulatory pathway linking a MIXTA-like transcription factor and NtZFP8 in trichome development. AmMIXTA does not directly regulate *NtZFP8* expression, as evidenced by DAP-seq results (Table S6). AmMIXTA and NtZFP8 significantly overlap in their directly regulated genes, with 45% of AmMIXTA targets also targeted by NtZFP8 and 77% of NtZFP8 targets also bound by AmMIXTA, indicating their joint or possibly antagonist role as transcriptional regulators. AmMIXTA was shown to bind to the GGTGGTGGTGG motif while NtZFP8 was found to bind the CTTCTTCTTCT motif (Fig. 5c, d).

Common targets bound in the promoter region identified by DAP-seq include *NtMYB6* and *NtGLABRA2* (Fig. 5f), whose homologs were characterized as involved in trichome development. For instance, *CsMYB6* is a negative regulator of trichome initiation in cucumber (Yang et al. 2018) while *AtGL2* and *CsGL2* promote trichome formation (Rerie et al. 1994; Cui et al. 2016). Interestingly, *SlGL2* is induced by SlSHINE3, which also regulates epidermal patterning and cuticle formation in tomato (Shi et al. 2013). In cucumber, CsGL3 (a HD-ZIP IV class protein) and CsGL1 (a HD-ZIP I class protein) interact to initiate multicellular trichome development, activating three regulators: CsGL2, CsMYB6, and CsWIN1/SHINE1 (Liu et al. 2016; Han et al. 2022). Their close tobacco homologs could be direct targets of AmMIXTA and/or NtZFP8 (Fig. 5f). *NtJACKDAW*, appearing also in the DAP-seq, could be of interest since in *Arabidopsis* its homolog is known to be required for the proper positioning of *AtGL2* expression, thereby ensuring correct root hair patterning (Hassan et al. 2010). Consistent with studies in *Arabidopsis* and *Cucumis sativus*(Rerie et al. 1994; Cui et al. 2016), which identified *GL2* as a key promoter of trichome formation, we observed that the *NtGL2* promoter is active in the stalk region of both glandular and non-glandular long-stalked trichomes (Fig. S7a). We further investigated the expression of *NtJACKDAW*, whose promoter activity closely mirrored that of *NtGL2* in trichomes (Fig. S7b). AmMIXTA was found to repress *NtJACKDAW* promoter activity while activating *NtGL2*. In contrast, *NtZFP8* functions as a positive regulator of *NtGL2*, but does not influence *NtJACKDAW*. Together, these results support a model in which AmMIXTA and NtZFP8 contribute to distinct layers of trichome transcriptional control and suggest that at least part of the transcriptional control regulating trichome development is evolutionarily conserved between species belonging to different plant families. We also advise caution against an overly simplistic view that each plant species has its own distinct transcriptional network governing the development of different trichome types. Our data highlight the fact that some components, like key regulatory modules are actually shared across species. This applies to both glandular and non-glandular trichomes, with genes like *ZFP8, GL2, MYB6, WOOLLY/PDF2* playing a role in regulating these processes in species as diverse as *N. tabacum, S. lycopersicum, C. sativus* or *A. thaliana*. This highlights the need to avoid assuming that all differences in trichome types come from distinct, independent regulatory networks. Instead, certain genetic elements are shared and reused in evolutionary adaptations, while others may evolve specifically in certain species.

In summary, our research leveraged the role of *AmMIXTA* to investigate the underlying transcriptional network controlling long-stalked glandular trichome formation. An endogenous MIXTA-like factor, still to be identified, is likely to interact with NtZFP8 in regulating this process. By partially revealing the complex transcriptional network behind this specific developmental mechanism, our findings lay the foundation for future studies aimed at identifying key genes and transcription factors driving or repressing trichome development in Solanaceae species. These investigations will explore signaling pathways, environmental influences, and the potential for targeted gene editing to optimize glandular trichome development, whether through induction or repression of this developmental process. This research could lead to practical applications in plant breeding programs that capitalize on these benefits for agricultural advancements.

Supplementary Information The online version contains supplementary material available at https://doi.org/10.1007/s00425-025-04840-9.

Acknowledgements We extend our sincerest gratitude to Prof. Beverley Glover for generously providing the cDNA of *AmMIXTA*, which was essential for the success of our experiments. We are also deeply thankful to Prof. Michel Ghislain for supplying the yeast two-hybrid system used in this study, to Prof. Jo Ecker for providing the genetic material required for the DAP-seq assay, to Aubry Fenestre for assistance in generating the reporter lines of the *NtGL2* promoter, and to Louis Gueuning for assistance with cloning of specific constructs.

We greatly appreciate their support and the invaluable resources they provided.

Author contributions AB conducted the foundational experiments for this study and drafted the manuscript. AR, MV, GW and MP were responsible for the creation of transgenic lines and the acquisition of preliminary transcriptomic data, AR participated in the drafting of a preliminary version of this manuscript. MP and GW performed the Yeast Two-Hybrid and the Dual Luciferase experiments. BEA and SL offered essential support in analyzing the RNA-seq and DAP-seq data. CH conceived and supervised the whole project and was actively involved in data analysis and writing of the manuscript.

Funding This work was supported by the Belgian National Fund for Scientific Research (PDR/PGY grant #T.0116.20 to AB, MP, GW and CH, FNRS Scientific Impulse Mandate # F.4522.17 to AR and MV, Charge de recherche #FC46171 to AB and FRIA #FC 58225 to GW) and the Swiss National Science Foundation (FNS; Grant#P2LAP3_191271 to AB). MV benefitted from funding from the UCLouvain Special Research Funds (UCLouvain FSR 2017).

Data availability RNA-seq and DAP-seq data sets are MIAME compliant and were submitted to the Gene Expression Omnibus (GEO) database under the GEO Series accession number GSE263485 and GSE263486.

Declarations

Conflict of interest The authors declare that there are no competing interests.

References

Bailey TL, Johnson J, Grant CE, Noble WS (2015) The MEME suite. Nucleic Acids Res 43(W1):W39–W49. https://doi.org/10.1093/nar/gkv416

Bartlett A, O'Malley RC, Huang S-sC, Galli M, Nery JR, Gallavotti A, Ecker JR (2017) Mapping genome-wide transcription-factor binding sites using DAP-seq. Nat Protoc 12(8):1659–1672. https://doi.org/10.1038/nprot.2017.055

Berhin A, de Bellis D, Franke RB, Buono RA, Nowack MK, Nawrath C (2019) The root cap cuticle: a cell wall structure for seedling establishment and lateral root formation. Cell 176(6):1367-1378.e1368. https://doi.org/10.1016/j.cell.2019.01.005

Bruex A, Kainkaryam RM, Wieckowski Y, Kang YH, Bernhardt C, Xia Y, Zheng X, Wang JY, Lee MM, Benfey P, Woolf PJ, Schiefelbein J (2012) A gene regulatory network for root epidermis cell differentiation in Arabidopsis. PLoS Genet 8(1):e1002446. https://doi.org/10.1371/journal.pgen.1002446

Chalvin C, Drevensek S, Dron M, Bendahmane A, Boualem A (2020) Genetic control of glandular trichome development. Trends Plant Sci 25(5):477–487. https://doi.org/10.1016/j.tplants.2019.12.025

Chang J, Yu T, Yang Q, Li C, Xiong C, Gao S, Xie Q, Zheng F, Li H, Tian Z, Yang C, Ye Z (2018) *Hair*, encoding a single C2H2 zinc-finger protein, regulates multicellular trichome formation in tomato. Plant J 96(1):90–102. https://doi.org/10.1111/tpj.14018

Chang J, Wu S, You T, Wang J, Sun B, Xu B, Xu X, Zhang Y, Wu S (2024) Spatiotemporal formation of glands in plants is modulated by MYB-like transcription factors. Nat Commun 15(1):2303. https://doi.org/10.1038/s41467-024-46683-0

Chen M, Ji M, Wen B, Liu L, Li S, Chen X, Gao D, Li L (2016) Golden 2-like transcription factors of plants. Front Plant Sci 7:1509. https://doi.org/10.3389/fpls.2016.01509

Chen Y, Su D, Li J, Ying S, Deng H, He X, Zhu Y, Li Y, Chen Y, Pirrello J, Bouzayen M, Liu Y, Liu M (2020) Overexpression of *bHLH95*, a basic helix–loop–helix transcription factor family member, impacts trichome formation via regulating gibberellin biosynthesis in tomato. J Exp Bot 71(12):3450–3462. https://doi.org/10.1093/jxb/eraa114

Cui J-Y, Miao H, Ding L-H, Wehner TC, Liu P-N, Wang Y, Zhang S-P, Gu X-F (2016) A new glabrous gene (*csgl3*) identified in trichome development in cucumber (*Cucumis sativus* L.). PLoS ONE 11(2):e0148422. https://doi.org/10.1371/journal.pone.0148422

Curtis MD, Grossniklaus U (2003) A gateway cloning vector set for high-throughput functional analysis of genes in planta. Plant Physiol 133(2):462–469. https://doi.org/10.1104/pp.103.027979

Ewas M, Gao Y, Wang S, Liu X, Zhang H, Nishawy EME, Ali F, Shahzad R, Ziaf K, Subthain H, Martin C, Luo J (2016) Manipulation of SlMXl for enhanced carotenoids accumulation and drought resistance in tomato. Sci Bull 61(18):1413–1418. https://doi.org/10.1007/s11434-016-1108-9

Gan Y, Liu C, Yu H, Broun P (2007) Integration of cytokinin and gibberellin signalling by *Arabidopsis* transcription factors GIS, ZFP8 and GIS2 in the regulation of epidermal cell fate. Development 134(11):2073–2081. https://doi.org/10.1242/dev.005017

Gantner J, Ordon J, Ilse T, Kretschmer C, Gruetzner R, Lofke C, Dagdas Y, Burstenbinder K, Marillonnet S, Stuttmann J (2018) Peripheral infrastructure vectors and an extended set of plant parts for the modular cloning system. PLoS ONE 13(5):e0197185. https://doi.org/10.1371/journal.pone.0197185

Gao S, Gao Y, Xiong C, Yu G, Chang J, Yang Q, Yang C, Ye Z (2017) The tomato b-type cyclin gene, *SlCycB2*, plays key roles in reproductive organ development, trichome initiation, terpenoids biosynthesis and *Prodenia litura* defense. Plant Sci 262:103–114. https://doi.org/10.1016/j.plantsci.2017.05.006

Gao S, Li N, Niran J, Wang F, Yin Y, Yu C, Jiao C, Yang C, Yao M (2021) Transcriptome profiling of *Capsicum annuum* using Illumina- and PacBio SMRT-based RNA-Seq for in-depth understanding of genes involved in trichome formation. Sci Rep 11:10164. https://doi.org/10.1038/s41598-021-89619-0

Gasparini K, Gasparini J, Therezan R, Vicente MH, Sakamoto T, Figueira A, Zsögön A, Peres LEP (2023) Natural genetic variation in the *HAIRS ABSENT* (*H*) gene increases type-VI glandular trichomes in both wild and domesticated tomatoes. J Plant Physiol 280:153859. https://doi.org/10.1016/j.jplph.2022.153859

Gershenzon J, Dudareva N (2007) The function of terpene natural products in the natural world. Nat Chem Biol 3(7):408–414. https://doi.org/10.1038/nchembio.2007.5

Glover BJ, Perez-Rodriguez M, Martin C (1998) Development of several epidermal cell types can be specified by the same MYB-related plant transcription factor. Development 125(17):3497–3508. https://doi.org/10.1242/dev.125.17.3497

Grefen C, Blatt MR (2012) A 2in1 cloning system enables ratiometric bimolecular fluorescence complementation (rBiFC). Biotechniques 53(5):311–314. https://doi.org/10.2144/000113941

Grunewald W, De Smet I, Lewis DR, Löfke C, Jansen L, Goeminne G, Vanden Bossche R, Karimi M, De Rybel B, Vanholme B, Teichmann T, Boerjan W, Van Montagu MCE, Gheysen G, Muday GK, Friml J, Beeckman T (2012) Transcription factor WRKY23 assists auxin distribution patterns during *Arabidopsis* root development through local control on flavonol biosynthesis. Proc Natl Acad Sci USA 109(5):1554–1559. https://doi.org/10.1073/pnas.1121134109

Han G, Wei X, Dong X, Wang C, Sui N, Guo J, Yuan F, Gong Z, Li X, Zhang Y, Meng Z, Chen Z, Zhao D, Wang B (2020) Arabidopsis ZINC FINGER PROTEIN1 acts downstream of GL2 to repress root hair initiation and elongation by directly suppressing bHLH genes. Plant Cell 32(1):206–225. https://doi.org/10.1105/tpc.19.00226

Han G, Li Y, Qiao Z, Wang C, Zhao Y, Guo J, Chen M, Wang B (2021) Advances in the regulation of epidermal cell development by C2H2 zinc finger proteins in plants. Front Plant Sci 12:754512. https://doi.org/10.3389/fpls.2021.754512

Han G, Li Y, Yang Z, Wang C, Zhang Y, Wang B (2022) Molecular mechanisms of plant trichome development. Front Plant Sci 13:910228. https://doi.org/10.3389/fpls.2022.910228

Hassan H, Scheres B, Blilou I (2010) Jackdaw controls epidermal patterning in the *Arabidopsis* root meristem through a non-cell-autonomous mechanism. Development 137(9):1523–1529. https://doi.org/10.1242/dev.048777

Hauser MT (2014) Molecular basis of natural variation and environmental control of trichome patterning. Front Plant Sci 5:320. https://doi.org/10.3389/fpls.2014.00320

Horsh RB, Fry JE, Hoffmann NL, Eichholtz D, Rogers SG, Fraley RT (1985) A simple and general method for transferring genes into plants. Science 227(4691):1229–1231. https://doi.org/10.1126/science.227.4691.1229

Huchelmann A, Boutry M, Hachez C (2017) Plant glandular trichomes: natural cell factories of high biotechnological interest. Plant Physiol 175(1):6–22. https://doi.org/10.1104/pp.17.00727

Ishida T, Hattori S, Sano R, Inoue K, Shirano Y, Hayashi H, Shibata D, Sato S, Kato T, Tabata S, Okada K, Wada T (2007) *Arabidopsis TRANSPARENT TESTA GLABRA2* is directly regulated by R2R3 MYB transcription factors and is involved in regulation of *GLABRA2* transcription in epidermal differentiation. Plant Cell 19(8):2531–2543. https://doi.org/10.1105/tpc.107.052274

Ishida T, Kurata T, Okada K, Wada T (2008) A genetic regulatory network in the development of trichomes and root hairs. Annu Rev Plant Biol 59(1):365–386. https://doi.org/10.1146/annurev.arplant.59.032607.092949

Jakoby MJ, Falkenhan D, Mader MT, Brininstool G, Wischnitzki E, Platz N, Hudson A, Hülskamp M, Larkin J, Schnittger A (2008) Transcriptional profiling of mature Arabidopsis trichomes reveals that *NOECK* encodes the MIXTA-like transcriptional regulator MYB106. Plant Physiol 148(3):1583–1602. https://doi.org/10.1104/pp.108.126979

Jin J, Tian F, Yang D-C, Meng Y-Q, Kong L, Luo J, Gao G (2017) Planttfdb 4.0: toward a central hub for transcription factors and regulatory interactions in plants. Nucleic Acids Res 45(D1):D1040–D1045. https://doi.org/10.1093/nar/gkw982

Karimi M, Inzé D, Depicker A (2002) Gateway™ vectors for *Agrobacterium*-mediated plant transformation. Trends Plant Sci 7(5):193–195. https://doi.org/10.1016/S1360-1385(02)02251-3

Khosla A, Paper JM, Boehler AP, Bradley AM, Neumann TR, Schrick K (2014) HD-Zip proteins GL2 and HDG11 have redundant functions in *Arabidopsis* trichomes, and GL2 activates a positive feedback loop via MYB23. Plant Cell 26(5):2184–2200. https://doi.org/10.1105/tpc.113.120360

Kirchmaier S, Lust K, Wittbrodt J (2013) Golden GATEway cloning – a combinatorial approach to generate fusion and recombination constructs. PLoS ONE 8(10):e76117. https://doi.org/10.1371/journal.pone.0076117

Lafuente MJ, Gancedo C, Jauniaux J-C, Gancedo JM (2000) Mth1 receives the signal given by the glucose sensors Snf3 and Rgt2 in *Saccharomyces cerevisiae*. Mol Microbiol 35(1):161–172. https://doi.org/10.1046/j.1365-2958.2000.01688.x

Law CW, Alhamdoosh M, Su S, Dong X, Tian L, Smyth GK, Ritchie ME (2016) RNA-seq analysis is easy as 1–2–3 with limma, Glimma and edgeR. F1000Research. https://doi.org/10.12688/f1000research.9005.3

Lin Q, Ohashi Y, Kato M, Tsuge T, Gu H, Qu L-J, Aoyama T (2015) GLABRA2 directly suppresses basic helix-loop-helix transcription factor genes with diverse functions in root hair development. Plant Cell 27(10):2894–2906. https://doi.org/10.1105/tpc.15.00607

Liu X, Bartholomew E, Cai Y, Ren H (2016) Trichome-related mutants provide a new perspective on multicellular trichome initiation and development in cucumber (*Cucumis sativus* L). Front Plant Sci 7:1187. https://doi.org/10.3389/fpls.2016.01187

Liu Y, Liu D, Khan AR, Liu B, Wu M, Huang L, Wu J, Song G, Ni H, Ying H, Yu H, Gan Y (2018) *Nbgis* regulates glandular trichome initiation through GA signaling in tobacco. Plant Mol Biol 98(1–2):153–167. https://doi.org/10.1007/s11103-018-0772-3

Matias-Hernandez L, Jiang W, Yang K, Tang K, Brodelius PE, Pelaz S (2017) AaMYB1 and its orthologue AtMYB61 affect terpene metabolism and trichome development in *Artemisia annua* and *Arabidopsis thaliana*. Plant J 90(3):520–534. https://doi.org/10.1111/tpj.13509

Meyberg M, Krohn S, Brümmer B, Kristen U (1991) Ultrastructure and secretion of glandular trichomes of tobacco leaves. Flora 185(5):357–363. https://doi.org/10.1016/S0367-2530(17)30495-4

Mi H, Muruganujan A, Huang X, Ebert D, Mills C, Guo X, Thomas PD (2019) Protocol update for large-scale genome and gene function analysis with the PANTHER classification system (v.14.0). Nat Protoc 14(3):703–721. https://doi.org/10.1038/s41596-019-0128-8

Nadakuduti SS, Pollard M, Kosma DK, Allen C, Ohlrogge JB, Barry CS (2012) Pleiotropic phenotypes of the *sticky peel* mutant provide new insight into the role of *CUTIN DEFICIENT2* in epidermal cell function in tomato. Plant Physiol 159(3):945–960. https://doi.org/10.1104/pp.112.198374

Noda K, Glover BJ, Linstead P, Martin C (1994) Flower colour intensity depends on specialized cell shape controlled by a Myb-related transcription factor. Nature 369(6482):661–664. https://doi.org/10.1038/369661a0

Paiano A, Margiotta A, De Luca M, Bucci C (2019) Yeast two-hybrid assay to identify interacting proteins. Curr Protoc Protein Sci 95(1):e70. https://doi.org/10.1002/cpps.70

Payne T, Clement J, Arnold D, Lloyd A (1999) Heterologous myb genes distinct from *GL1* enhance trichome production when overexpressed in *Nicotiana tabacum*. Development 126(4):671–682. https://doi.org/10.1242/dev.126.4.671

Payne CT, Zhang F, Lloyd AM (2000) *GL3* encodes a bHLH protein that regulates trichome development in Arabidopsis through interaction with GL1 and TTG1. Genetics 156(3):1349–1362. https://doi.org/10.1093/genetics/156.3.1349

Perez-Rodriguez M, Jaffe FW, Butelli E, Glover BJ, Martin C (2005) Development of three different cell types is associated with the activity of a specific MYB transcription factor in the ventral petal of *Antirrhinum majus* flowers. Development 132(2):359–370. https://doi.org/10.1242/dev.01584

Plett JM, Wilkins O, Campbell MM, Ralph SG, Regan S (2010) Endogenous overexpression of *Populus MYB186* increases trichome density, improves insect pest resistance, and impacts plant growth.

Plant J 64(3):419–432. https://doi.org/10.1111/j.1365-313X.2010.04343.x

Qi X, Chen Z, Yu X, Li L, Bai Y, Fang H, Liang C (2022) Characterisation of the *Mentha canadensis* R2R3-MYB transcription factor gene *McMIXTA* and its involvement in peltate glandular trichome development. BMC Plant Biol 22(1):219–219. https://doi.org/10.1186/s12870-022-03614-9

Rauluseviciute I, Riudavets-Puig R, Blanc-Mathieu R, Castro-Mondragon Jaime A, Ferenc K, Kumar V, Lemma RB, Lucas J, Chèneby J, Baranasic D, Khan A, Fornes O, Gundersen S, Johansen M, Hovig E, Lenhard B, Sandelin A, Wasserman Wyeth W, Parcy F, Mathelier A (2024) JASPAR 2024: 20th anniversary of the open-access database of transcription factor binding profiles. Nucleic Acids Res 52(D1):D174–D182. https://doi.org/10.1093/nar/gkad1059

Rerie WG, Feldmann KA, Marks MD (1994) The GLABRA2 gene encodes a homeo domain protein required for normal trichome development in Arabidopsis. Genes Dev 8(12):1388–1399. https://doi.org/10.1101/gad.8.12.1388

Sayols S (2023) rrvgo: a bioconductor package for interpreting lists of gene ontology terms. MicroPubl Biol. https://doi.org/10.17912/micropub.biology.000811

Schmittgen TD, Livak KJ (2008) Analyzing real-time PCR data by the comparative CT method. Nat Protoc 3(6):1101–1108. https://doi.org/10.1038/nprot.2008.73

Shi JX, Adato A, Alkan N, He Y, Lashbrooke J, Matas AJ, Meir S, Malitsky S, Isaacson T, Prusky D, Leshkowitz D, Schreiber L, Granell AR, Widemann E, Grausem B, Pinot F, Rose JK, Rogachev I, Rothan C, Aharoni A (2013) The tomato SlSHINE3 transcription factor regulates fruit cuticle formation and epidermal patterning. New Phytol 197(2):468–480. https://doi.org/10.1111/nph.12032

Shi P, Fu X, Shen Q, Liu M, Pan Q, Tang Y, Jiang W, Lv Z, Yan T, Ma Y, Chen M, Hao X, Liu P, Li L, Sun X, Tang K (2017) The roles of AaMIXTA1 in regulating the initiation of glandular trichomes and cuticle biosynthesis in *Artemisia annua*. New Phytol 217(1):261–276. https://doi.org/10.1111/nph.14789

Shi X, Gu Y, Dai T, Wu Y, Wu P, Xu Y, Chen F (2018) Regulation of trichome development in tobacco by *JcZFP8*, a C2H2 zinc finger protein gene from *Jatropha curcas* L. Gene 658:47–53. https://doi.org/10.1016/j.gene.2018.02.070

Sierro N, Battey JND, Ouadi S, Bakaher N, Bovet L, Willig A, Goepfert S, Peitsch MC, Ivanov NV (2014) The tobacco genome sequence and its comparison with those of tomato and potato. Nat Commun 5:3833. https://doi.org/10.1038/ncomms4833

Sun L, Zhang A, Zhou Z, Zhao Y, Yan A, Bao S, Yu H, Gan Y (2015) *Glabrous inflorescence stems3* (*GIS3*) regulates trichome initiation and development in *Arabidopsis*. New Phytol 206(1):220–230. https://doi.org/10.1111/nph.13218

Thomas PD, Ebert D, Muruganujan A, Mushayahama T, Albou L-P, Mi H (2022) PANTHER: making genome-scale phylogenetics accessible to all. Protein Sci 31(1):8–22. https://doi.org/10.1002/pro.4218

Tissier A (2012) Glandular trichomes: what comes after expressed sequence tags? Plant J 70(1):51–68. https://doi.org/10.1111/j.1365-313X.2012.04913.x

Uzelac B, Stojičić D, Budimir S (2021) Glandular trichomes on the leaves of *Nicotiana tabacum*: morphology, developmental ultrastructure, and secondary metabolites. In: Ramawat KG, Ekiert HM, Goyal S (eds) Plant cell and tissue differentiation and secondary metabolites: fundamentals and applications. Springer International Publishing, Cham, pp 25–61. https://doi.org/10.1007/978-3-030-30185-9_1

Vandesompele J, De Preter K, Pattyn F, Poppe B, Van Roy N, De Paepe A, Speleman F (2002) Accurate normalization of real-time quantitative RT-PCR data by geometric averaging of multiple internal control genes. Genome Biol. https://doi.org/10.1186/gb-2002-3-7-research0034

Wang L, Zhou C-M, Mai Y-X, Li L-Z, Gao J, Shang G-D, Lian H, Han L, Zhang T-Q, Tang H-B, Ren H, Wang F-X, Wu L-Y, Liu X-L, Wang C-S, Chen E-W, Zhang X-N, Liu C, Wang J-W (2019) A spatiotemporally regulated transcriptional complex underlies heteroblastic development of leaf hairs in *Arabidopsis thaliana*. EMBO J 38(8):e100063. https://doi.org/10.15252/embj.2018100063

Wang Z, Yan X, Zhang H, Meng Y, Pan Y, Cui H (2021) *NtCycB2* negatively regulates tobacco glandular trichome formation, exudate accumulation, and aphid resistance. Plant Mol Biol 108:65–76. https://doi.org/10.1007/s11103-021-01222-z

Wu ML, Cui YC, Ge L, Cui LP, Xu ZC, Zhang HY, Wang ZJ, Zhou D, Wu S, Chen L, Cui H (2020) NbCycB2 represses Nbwo activity via a negative feedback loop in tobacco trichome development. J Exp Bot 71:1815–1827. https://doi.org/10.1093/jxb/erz542

Wu M, Chang J, Han X, Shen J, Yang L, Hu S, Huang B-B, Xu H, Xu M, Wu S, Li P, Hua B, Yang M, Yang Z, Wu S (2023) A HD-ZIP transcription factor specifies fates of multicellular trichomes via dosage-dependent mechanisms in tomato. Dev Cell 58(4):278-288.e275. https://doi.org/10.1016/j.devcel.2023.01.009

Wu M, Bian X, Hu S, Huang B, Shen J, Du Y, Wang Y, Xu M, Xu H, Yang M, Wu S (2024a) A gradient of the HD-Zip regulator Woolly regulates multicellular trichome morphogenesis in tomato. Plant Cell 36(6):2375–2392. https://doi.org/10.1093/plcell/koae077

Wu R, Liu Z, Sun S, Qin A, Liu H, Zhou Y, Li W, Liu Y, Hu M, Yang J, Rochaix J-D, An G, Herrera-Estrella L, Tran L-SP, Sun X (2024b) Identification of bZIP transcription factors that regulate the development of leaf epidermal cells in *Arabidopsis thaliana* by single-cell RNA sequencing. Int J Mol Sci 25(5):2553. https://doi.org/10.3390/ijms25052553

Xie L, Yan T, Li L, Chen M, Ma Y, Hao X, Fu X, Shen Q, Huang Y, Qin W, Liu H, Chen T, Hassani D, Kayani S-l, Rose JKC, Tang K (2021) The WRKY transcription factor AaGSW2 promotes glandular trichome initiation in *Artemisia annua*. J Exp Bot 72(5):1691–1701. https://doi.org/10.1093/jxb/eraa523

Xu J, van Herwijnen ZO, Drager DB, Sui C, Haring MA, Schuurink RC (2018) SlMYC1 regulates type VI glandular trichome formation and terpene biosynthesis in tomato glandular cells. Plant Cell 30(12):2988–3005. https://doi.org/10.1105/tpc.18.00571

Yan T, Chen M, Shen Q, Li L, Fu X, Pan Q, Tang Y, Shi P, Lv Z, Jiang W, Ma Y-n, Hao X, Sun X, Tang K (2017) Homeodomain protein 1 is required for jasmonate-mediated glandular trichome initiation in *Artemisia annua*. New Phytol 213(3):1145–1155. https://doi.org/10.1111/nph.14205

Yan T, Li L, Xie L, Chen M, Shen Q, Pan Q, Fu X, Shi P, Tang Y, Huang H, Huang Y, Huang Y, Tang K (2018) A novel HD-ZIP IV/MIXTA complex promotes glandular trichome initiation and cuticle development in *Artemisia annua*. New Phytol 218(2):567–578. https://doi.org/10.1111/nph.15005

Yang C, Li H, Zhang J, Wang T, Ye Z (2011) Fine-mapping of the woolly gene controlling multicellular trichome formation and embryonic development in tomato. Theor Appl Genet 123(4):625–633. https://doi.org/10.1007/s00122-011-1612-x

Yang C, Gao Y, Gao S, Yu G, Xiong C, Chang J, Li H, Ye Z (2015) Transcriptome profile analysis of cell proliferation molecular processes during multicellular trichome formation induced by tomato *Wo*^{v} gene in tobacco. BMC Genomics 16:868. https://doi.org/10.1186/s12864-015-2099-7

Yang S, Cai Y, Liu X, Dong M, Zhang Y, Chen S, Zhang W, Li Y, Tang M, Zhai X, Weng Y, Ren H (2018) A *CsMYB6-CsTRY*

module regulates fruit trichome initiation in cucumber. J Exp Bot 69(8):1887–1902. https://doi.org/10.1093/jxb/ery047

Zhang F, Gonzalez A, Zhao M, Payne CT, Lloyd A (2003) A network of redundant bHLH proteins functions in all TTG1-dependent pathways of *Arabidopsis*. Development 130(20):4859–4869. https://doi.org/10.1242/dev.00681

Zheng F, Cui L, Li C, Xie Q, Ai G, Wang J, Yu H, Wang T, Zhang J, Ye Z, Yang C (2021) Hair (H) interacts with SlZFP8-like to regulate the initiation and elongation of trichomes by modulating *SlZFP6* expression in tomato. J Exp Bot 73:228–244. https://doi.org/10.1093/jxb/erab417

Zhou Z, Sun L, Zhao Y, An L, Yan A, Meng X, Gan Y (2013) *Zinc finger protein 6* (*ZFP6*) regulates trichome initiation by integrating gibberellin and cytokinin signaling in *Arabidopsis thaliana*. New Phytol 198(3):699–708. https://doi.org/10.1111/nph.12211